JNeurosci
THE JOURNAL OF NEUROSCIENCE

Research Articles: Systems/Circuits

Temporal contingencies determine whether adaptation strengthens or weakens normalization

A Aschner[1], SG Solomon[2], MS Landy[3], DJ Heeger[3] and A Kohn[1,4,5]

[1]*Dominik Purpura Dept. of Neuroscience, Albert Einstein College of Medicine, Bronx NY 10461*
[2]*Dept. of Experimental Psychology, UCL, London UK WC1H 0AP*
[3]*Dept. of Psychology & Center for Neural Science, NYU, New York NY 10003*
[4]*Dept. of Ophthalmology and Visual Sciences, Albert Einstein College of Medicine Bronx NY 10461*
[5]*Dept. of Systems and Computational Biology, Albert Einstein College of Medicine Bronx NY 10461*

DOI: 10.1523/JNEUROSCI.1131-18.2018

Received: 4 May 2018

Revised: 30 August 2018

Accepted: 19 September 2018

Published: 5 October 2018

Author contributions: A.A., S.S., M.S.L., D.J.H., and A.K. designed research; A.A. and A.K. performed research; A.A. and A.K. analyzed data; A.A. wrote the first draft of the paper; A.A., S.S., M.S.L., D.J.H., and A.K. edited the paper; A.A., S.S., M.S.L., D.J.H., and A.K. wrote the paper.

Conflict of Interest: The authors declare no competing financial interests.

We thank Christopher Henry, Selina Solomon, and Thad Czuba for assistance with data collection and Ruben Coen-Cagli for helpful comments and discussions. This work was supported by NIH EY016774 (AK), NIH EY08266 (MSL), Stavros Niarchos Foundation/Research to Prevent Blindness (SGS and AK), FP7 618661 (SGS), and the Hirschl/Weill-Caulier Trust (AK).

Corresponding author: Amir Aschner, Dept. of Neuroscience, Albert Einstein College of Medicine, 1410 Pelham Parkway South, Room 822, Bronx NY 10461, aaschner@mail.einstein.yu.edu

Cite as: J. Neurosci ; 10.1523/JNEUROSCI.1131-18.2018

Temporal contingencies determine whether adaptation strengthens or weakens normalization

Aschner A[1], Solomon SG[2], Landy MS[3], Heeger DJ[3], Kohn A[1,4,5]

1 Dominik Purpura Dept. of Neuroscience, Albert Einstein College of Medicine, Bronx NY 10461;
2 Dept. of Experimental Psychology, UCL, London UK WC1H 0AP;
3 Dept. of Psychology & Center for Neural Science, NYU, New York NY 10003
4 Dept. of Ophthalmology and Visual Sciences, Albert Einstein College of Medicine Bronx NY 10461;
5 Dept. of Systems and Computational Biology, Albert Einstein College of Medicine Bronx NY 10461;

Abbreviated title: Adaptation-induced changes in normalization

Author Contributions:
Designed experiment: Aschner A, Solomon SG, Landy MS, Heeger DJ, Kohn A
Collected data: Aschner A, Kohn A
Analyzed data: Aschner A, Kohn A
Wrote paper: Aschner A, Solomon SG, Landy MS, Heeger DJ, Kohn A

Corresponding author:
Amir Aschner
Dept. of Neuroscience
Albert Einstein College of Medicine
1410 Pelham Parkway South, Room 822
Bronx NY 10461
aaschner@mail.einstein.yu.edu

Number of pages: 39
Number of figures: 8
Number of tables: 0
Number of multimedia: 0
Number of 3-d models: 0

Abstract word count: 246
Introduction word count: 509
Discussion word count: 1906

Conflict of interest: The authors declare no competing financial interests.

Acknowledgements: We thank Christopher Henry, Selina Solomon, and Thad Czuba for assistance with data collection and Ruben Coen-Cagli for helpful comments and discussions. This work was supported by NIH EY016774 (AK), NIH EY08266 (MSL), Stavros Niarchos Foundation/Research to Prevent Blindness (SGS and AK), FP7 618661 (SGS), and the Hirschl/Weill-Caulier Trust (AK).

ABSTRACT

A fundamental and nearly ubiquitous feature of sensory encoding is that neuronal responses are strongly influenced by recent experience, or adaptation. Theoretical and computational studies have proposed that many adaptation effects may result, in part, from changes in the strength of normalization signals. Normalization is a 'canonical' computation in which a neuron's response is modulated (normalized) by the pooled activity of other neurons. Here we test whether adaptation can alter the strength of cross-orientation suppression, or masking, a paradigmatic form of normalization evident in primary visual cortex (V1). We made extracellular recordings of V1 neurons in anesthetized male macaques, and measured responses to plaid stimuli composed of two overlapping, orthogonal gratings, before and after prolonged exposure to two distinct adapters. The first adapter was a plaid consisting of orthogonal gratings, and led to stronger masking. The second adapter presented the same orthogonal gratings in an interleaved manner, and led to weaker masking. The strength of adaptation's effects on masking depended on the orientation of the test stimuli relative to the orientation of the adapters, but was independent of neuronal orientation preference. Changes in masking could not be explained by altered neuronal responsivity. Our results suggest that normalization signals can be strengthened or weakened by adaptation, depending on the temporal contingencies of the adapting stimuli. Our findings reveal an interplay between two widespread computations in cortical circuits—adaptation and normalization—that enables flexible adjustments to the structure of the environment, including the temporal relationships among sensory stimuli.

SIGNIFICANCE STATEMENT

Two fundamental features of sensory responses are that they are influenced by adaptation, and that they are modulated by the activity of other nearby neurons via normalization. Our findings reveal a strong interaction between these two aspects of cortical computation. Specifically, we show that cross-orientation masking—a form of normalization—can be strengthened or weakened by adaptation, depending on the temporal contingencies between sensory inputs. Our findings support theoretical proposals that some adaptation effects may involve altered normalization, and offer a network-based explanation for how cortex adjusts to current sensory demands.

INTRODUCTION

Sensory statistics vary over time, imposing changing demands on the brain. Sensory neuronal responses adjust to the recent pattern of inputs, or adaptation. This adjustment is a fundamental and nearly ubiquitous feature of sensory encoding (Clifford et al., 2007; Kohn, 2007; Schwartz et al., 2007; Wark et al., 2007; Rieke and Rudd, 2009; Solomon and Kohn, 2014; Webster, 2015).

Adaptation has diverse effects on sensory neurons, including changes in responsivity and altered tuning or selectivity (see Solomon and Kohn, 2014 for review). Theoretical and computational work has proposed that much adaptation phenomenology could be explained through adjustments of normalization signals (Heeger, 1992; Wainwright et al., 2002; Lochmann et al., 2012; Solomon and Kohn, 2014; Snow et al., 2016; Westrick et al., 2016). Normalization is a 'canonical' computation, in which a neuron's response is divisively modulated by the activity of other neurons, a normalization pool (Heeger, 1992; Carandini and Heeger, 2012). Normalization can explain non-linear response properties of cortical visual neurons, such as cross-orientation suppression (hereafter, masking; Morrone et al., 1982; Carandini et al., 1997a; Priebe and Ferster, 2006) and spatial contextual effects (surround suppression; Cavanaugh et al., 2002; Coen-Cagli et al., 2012, 2015). Normalization has also been invoked to explain phenomena as varied as olfactory encoding in *Drosophila* and value encoding in primates (Carandini and Heeger, 2012).

Previous work has provided some evidence that adaptation alters the suppression attributed to normalization. For instance, adaptation of the receptive field surround weakens the suppression it provides in the lateral geniculate nucleus (LGN) and primary visual cortex (V1), leading to response facilitation (Webb et al., 2005; Camp et al., 2009; Wissig and Kohn, 2012; Patterson et al., 2013). How adaptation affects masking within the receptive field is unclear. One study found masking was unaltered in V1 after adaptation (Freeman et al., 2002), but others reported it was weakened (Li et al., 2005; Dhruv et al., 2011; see also Kaliukhovich and Vogels, 2016). Critically, no systematic study has reported that the suppression attributed to normalization can be strengthened

by adaptation. The ability of recent sensory experience to strengthen normalization is a critical component of most normalization-based models of adaptation effects.

The Hebbian normalization model (Westrick et al., 2016) was proposed to explain adaptation effects in visual cortex, and provides clear predictions about when normalization should be strengthened or weakened by adaptation. Specifically, it predicts that changes in normalization signals between neurons depend on their recent history of co-activation (also see Barlow and Földiák, 1989; Wainwright et al., 2002 and Hosoya et al., 2005 for related suggestions). When the normalization pool and a target neuron are consistently co-active, normalization should be strengthened. Conversely, when the neuron and normalization pool are driven asynchronously, normalization should be weakened.

We tested these predictions using extracellular recordings of macaque V1 neurons. We compared the strength of masking before and after consistent pairing of a target grating and mask (contingent adaptation), or the asynchronous presentation of these stimuli. We show that masking can be strengthened or weakened, depending on whether mask and target are consistently paired or separated in time.

MATERIALS AND METHODS

Surgery: We made recordings from 5 adult male macaque monkeys (*Macaca fascicularis*). Animals were administered glycopyrrolate (0.01 mg/kg) and diazepam (1.5 mg/kg) shortly before the induction of anesthesia with ketamine (10 mg/kg). Animals were then intubated and provided isoflurane (1-2%). Intravenous catheters were placed in the saphenous veins of each leg. Animals were positioned in a stereotaxic device and a craniotomy and durotomy were performed over V1 (approximately 5 mm posterior to the lunate sulcus and 10 mm lateral to the midline). A 10x10 microelectrode array (400 μm spacing, 1 mm length; Blackrock Microsystems) was implanted and the craniotomy was covered with agar to prevent desiccation. Post-surgical anesthesia was maintained with a venous infusion of sufentanil citrate (6-24 μg/kg/hr, adjusted as needed) in Normosol solution with dextrose. Vecuronium

bromide (150 µg/kg/hr) was provided intravenously to minimize eye movements. Vital signs, including heart rate, $Sp0_2$, ECG, blood pressure, EEG, end-tidal CO_2 partial pressure, core temperature, urinary output, and airway pressure were constantly monitored to ensure adequate anesthesia and physiological state. Heating pads maintained rectal temperature near 37˚ Celsius. Topical atropine was used to dilate the pupils. Corneas were protected with gas-permeable contact lenses. Supplementary lenses were used to bring the retinal image into focus. Antibiotics (Baytril, 2.5 mg/kg) and a corticosteroid (dexamethasone, 1 mg/kg) were administered daily.

All procedures were approved by the Institutional Animal Care and Use Committee of the Albert Einstein College of Medicine and were in compliance with the guidelines set forth in the National Institutes of Health *Guide for the Care and Use of Laboratory Animals*.

Recording and visual stimuli: Extracellular voltage signals were filtered from 0.5-7.5 kHZ. Waveforms that exceeded a user-defined voltage threshold (usually 5 times the root-mean-square signal on each channel) were digitized at 30 kHz. Waveforms were classified using the Plexon Offline Sorter into single- and multi-unit clusters. We computed signal-to-noise ratios (SNRs) for each unit as the ratio of the amplitude of the average waveform to the standard deviation of the individual waveforms (Kelly et al., 2007). Units with an SNR ≥ 3.5 were classified as single units. Results were similar for these single units (13% of units) and for multi-unit clusters and are therefore presented together (see also Wissig and Kohn, 2012). Due to the duration of the adaptation experiments—roughly two hours—each recording was sorted separately.

Visual stimuli were generated with custom software based on OpenGL (EXPO; P. Lennie) and displayed on a calibrated cathode ray tube monitor (HP p1230; 1024 x 768 pixels; 100 Hz frame rate, ~40 cd/m^2 mean luminance), viewed at a distance of 110 cm and subtending ~20˚ of visual angle. Spatial receptive fields (RFs) of each unit were estimated by occluding one eye and presenting small patches of drifting gratings (0.5˚ diameter; 4 orientations, 1 cycle/˚, 3 Hz drift rate, 250 ms presentation) at 225 distinct

positions spanning a 3˚ x 3˚ region of visual space. Subsequent stimuli were centered in the aggregate RF of the recorded units.

Stimulus orientations for subsequent experiments were determined by presenting a continuous, pseudorandom sequence of 16 full-contrast sinusoidal gratings (1.5˚ patch diameter, 1 cycle/˚, 3 Hz drift rate) at equally spaced orientations (22.5˚ steps; 1 s presentation). Gratings were presented monocularly, in a hard-edged circular window.

To characterize normalization, we measured masking (or cross-orientation suppression; Morrone et al., 1982; Bonds, 1989; DeAngelis et al., 1992; Carandini et al., 1997a) by presenting a drifting, sinusoidal grating (the target) with an overlapping, orthogonal grating (the mask). Both gratings were presented monocularly, in a hard-edged circular window 1.5˚ in diameter, with a spatial frequency of 1.5 cycle/˚ and drift rate of 3 Hz. On each trial the contrast of the target and mask gratings varied independently over 5 values (0%, 6.25%, 12.5%, 25% and 50%), generating a matrix of 25 test stimuli (Figure 1A). For each neuron, we defined the target as the grating that evoked the stronger response at 50% contrast when presented alone.

<Figure 1: Stimuli>

To measure the strength of masking in control conditions (i.e., before adaptation), we used 1 s presentations of each of the 25 test stimuli, interleaved with 5 s presentations of a uniform gray screen (Figure 1C). The order of presentation was randomized within each block of trials and each stimulus was presented 20 times. We refer to these as pre-adaptation responses, though they are more accurately termed responses measured during adaptation to a gray, uniform screen. We then measured responses after adaptation, using an ‘adapt-test-top-up’ paradigm (Figure 1C; Kohn and Movshon, 2004). After 40 s of initial exposure to the adapter, we presented each of the 25 test stimuli for 1 s (block randomized, as above), interleaved with 5 s presentations of the adapter. Each stimulus was presented 20 times.

We used two types of adapters (Figure 1B). For asynchronous adaptation, the target and mask grating (each 50% contrast) alternated in time, with each drifting grating displayed for 250 ms and no inter-stimulus interval. For contingent adaptation the same two gratings were presented simultaneously (forming a plaid) for 250 ms, alternated with 250 ms of a uniform gray screen. The presentation of a blank screen between plaids ensured the time-averaged contrast of each adapter type was equal between adaptation paradigms.

To assess the stimulus (orientation) specificity of adaptation effects, we measured responses to mask and target stimuli that were rotated relative to the adapter by 45° (e.g., the effects of adaptation to 0-90° plaids were evaluated with 45-135° plaids).

Finally, to determine how adaptation effects depended on the orientation preference of the recorded unit, we conducted additional experiments in which masking was measured with a reduced test-stimulus ensemble, combined with interleaved presentations of gratings of different orientations. Specifically, we presented the target and mask at contrasts of 0%, 6.25%, 12.5%, 25% and 50%, either in isolation or paired with the 50% contrast orthogonal grating. Tuning was measured with 50% contrast gratings spanning 180° of orientation in 22.5° steps. The temporal structure of these experiments was identical to that described above.

Analyses: Data analysis was performed in MATLAB (MathWorks). We measured responses for two cycles of the grating (666 ms), beginning 333 ms after stimulus onset. For each neuron, we measured both the mean response (F0) and its modulation by the grating drift frequency (F1), for the high-contrast target. We used the response measure (F0 or F1) that gave the higher value for all subsequent analyses.

We quantified masking strength with an index based on the area-under-the-curve (AUC) of the contrast response functions for the target grating, in the presence and absence of the mask (similar to Carandini et al., 1997b,1998; Wissig and Kohn, 2012; using log contrast values as the x-axis except for the placement of zero contrast, as in Figure 2).

We used this approach, rather than fitting descriptive functions to the data (as in Freeman et al., 2002; Dhruv et al., 2011), because post-adaptation responses often showed little evidence of contrast saturation, leaving model parameters poorly constrained by the data.

We measured the AUC for each mask contrast separately (AUC_{TM}), after subtracting the response to the mask when presented alone. The AUC for the target alone (AUC_T) was that obtained for masks of zero contrast. Negative AUC_{TM} values were set to zero, so that our masking index was constrained to lie between -1 and 1. The masking index was defined as:

$$MI = \frac{(AUC_T - AUC_{TM})}{(AUC_T + AUC_{TM})} \quad \text{(Eq. 1)}$$

A masking index near 1 indicates strong masking ($AUC_T >> AUC_{TM}$), whereas a value near 0 indicates little masking ($AUC_T \approx AUC_{TM}$). Negative values indicate that the response to the target alone (AUC_T) was smaller than the difference between the response to the plaid and the response to the mask alone (AUC_{TM}).

To ensure we could measure masking, if it occurred, we only analyzed data from cells for which the response to the 50% contrast target was greater than the mean + 3 standard errors of the mean (SEM) of the spontaneous firing rate, both before and after adaptation (38% of units excluded for contingent-adaptation experiments; 57% for asynchronous adaptation). The relatively high proportion of excluded units arose because we presented gratings at only two orientations, and one spatial and temporal frequency. Thus, these stimuli failed to drive robust responses in many of the recorded units.

Note that more units were excluded for asynchronous adaptation experiments than for contingent adaptation, because responses were more strongly reduced after asynchronous adaptation (Figures 4 and 5). Further, we found that units with particularly weak responses after adaptation tended to have higher pre-adaptation masking indices. As a result, the pre-adaptation masking index was lower for asynchronous than contingent adapters among the units analyzed. To ensure that this

mismatch in pre-adaptation masking index did not contribute to the observed differences in the effects of contingent and asynchronous adaptation, we repeated our analyses after matching the pre-adaptation masking indices for the two data sets. Specifically, we binned the pre-adaptation masking indices (bin width of 0.2) in each data set, and then randomly selected for each bin the same number of units in the two data sets. This matching led to pre-adaptation masking values that were statistically indistinguishable. All of the differences between the effects of contingent and asynchronous adaptation that are reported in the manuscript were equally evident in this subset of data (data not shown).

To control for any confounds due to adaptation-induced changes in responsivity, we performed additional analyses. We first calculated a suppression index from the post-adaptation responses defined as:

$$SI = 1 - \frac{R_{TM}}{R_T + R_M} \quad \text{(Eq. 2)}$$

where R_T and R_M are the responses to the 50% contrast target and mask, respectively, and R_{TM} is the response to the two presented together (i.e., the plaid).

We then identified target and mask contrasts in the pre-adaptation condition that produced responses equivalent to those observed after adaptation. To do so, we needed to interpolate the pre-adaptation measurements, so we fitted those data for each cell with a descriptive function:

$$B + \frac{(A_T * T_c + A_M * M_c)^n}{1 + (d_T * T_c)^n + (d_M * M_c)^n} \quad \text{(Eq. 3)}$$

where T_c and M_c are the contrasts of the target and mask, respectively; B is the spontaneous firing rate; A_T and A_M determine the drive provided by each grating; n approximates an expansive nonlinearity; and d_T and d_M capture the weight of each grating in the normalization signal. These parameters (A_T, A_M, d_T, d_M, and n) were estimated by maximizing the log likelihood of the data given the model predictions, assuming Poisson spiking statistics (El-Shamayleh and Movshon, 2011). Fit quality was characterized by the normalized log likelihood, where the lower bound (a value of 0) was the likelihood of a model with predicted responses equal to the average response

across all conditions, and the upper bound (a value of 1) was the likelihood calculated by using the data as the model (Stocker and Simoncelli, 2006). The mean fit quality of the analyzed units (see below) was 0.86.

We used the model fit to (1) identify contrasts of the target and mask that generated predicted responses equal to those observed after adaptation [R_T and R_M of Eq. 2]; and (2) estimate responses to plaid stimuli composed of the target and mask at these 'rate-matched' contrasts. We then calculated a pre-adaptation rate-matched suppression index (SI), as in Eq. 2, from these responses. This analysis allowed us to compare SI values before and after adaptation for which, by definition, responsivity to the component gratings was equal. Thus, we could compare how summation was affected by adaptation, when the efficacy of the individual gratings was identical before and after adaptation.

For this analysis, we included units only if: (1) The pre- and post-adaptation responses to both the 50% contrast mask and the 50% target were at least 3 SEMs above the mean spontaneous rate, since we could only measure summation for mean-matched responses when both stimuli generated measurable responses. This criterion excluded 57% of units in the contingent-adaptation experiment, and 77% in the asynchronous-adaptation experiments. (2) The model fit quality to the pre-adaptation data was at least 0.7, so that the matching to pre-adaptation responses was meaningful (18% of remaining units excluded). (3) We could identify a contrast that evoked a matched response in the pre-adaptation epoch (30% of the remaining units excluded). Because of these requirements, we were able to perform this analysis on 12% of the recorded units.

To estimate neuronal orientation preference, we fitted the responses to gratings spanning a 180° range of orientations with a von Mises function, using the maximum-likelihood fitting procedure described above. To ensure that our measurements of preference were meaningful, we only analyzed responses for which fit quality exceeded 0.7 (mean fit quality of selected neurons was 0.86). We also used the fitted functions to

estimate tuning-curve gain, before and after adaptation, defined as the maximum predicted evoked response.

To quantify statistical significance, we used *t*-tests (two-tailed), unless otherwise indicated. All error estimates indicate one standard error from the mean, unless indicated otherwise.

Response-product homeostasis model: We performed simulations to compare our neurophysiological results to those predicted by a recently proposed rule for updating normalization weights based on stimulus history ('Hebbian normalization model' of Westrick et al., 2016).

Our variant of the Hebbian normalization model consisted of 120 neurons with preferred orientations equally spaced from 0-178.5°. Responses were simulated by computing a feedforward drive for each neuron, and then normalizing by the feedforward drive to the other neurons. Specifically, the feedforward drive for cell *i* was defined as:

$$F_i(\theta) = C * \exp[k * \cos(\theta - \theta_i) - 1] + B \quad \text{(Eq.4)}$$

where θ is the grating orientation and C is its contrast, θ_i is the preferred orientation of cell i, and B is an offset. The response of the cell was then computed as:

$$R_i(\theta) = \frac{F_i(\theta)^2}{\sigma^2 + \sum_{j=1}^{N} W_{i,j} F_j(\theta)^2} \quad \text{(Eq. 5)}$$

where W_{ij} is the weight which defines unit j's contribution to i's normalization pool; and σ is the contrast saturation constant.

The normalization weight between each pair of neurons was updated based on their responses to the current stimulus:

$$W_{i,j}^{t+1} = W_{i,j}^{t} + \alpha(R_i^t R_j^t - H_{i,j}) \quad \text{(Eq. 6)}$$

where α is a factor that determines the update rate, and $H_{i,j}$ is a homeostatic target defined as the mean response product of the pair.

We also considered a variant of the model which included a 'fatigue' factor, which was defined as:

$$G_i^{t+1} = G_i^t + \beta(R_i^t / Rmax_i) \quad \text{(Eq 7)}$$

where $Rmax_i$ is the response of the neuron to its preferred grating at full contrast. The response of each neuron, R_i as defined in Eq. 5, were then scaled by 1-G_i, at each time step. The initial value of G_i was 0, for all units.

For the model simulations without fatigue (Figures 6 and 7), we used the following parameters: k was 3, producing a bandwidth (full width at half height) of ~40°; B was 0.1, σ was 0.35; α was 0.005; $H_{i,j}$ was defined as the mean of the pre-adaptation response product of the pair to gratings of all orientation presented at 36% contrast; the initial normalization weights were 0.027; and the model was run for 200 time steps. For the simulations with fatigue (Figure 7), the parameters were as above, except: B was 0.3; α was 0.01, $H_{i,j}$ was defined with gratings at 50% contrast; and the model was run for 1000 time steps. For fatigue, the parameter β was set to 0.015 and values of G>0.55 were set to 0.55.

Code Availability: All Matlab code and analysis will be made available upon reasonable request to the corresponding author.

RESULTS

We recorded neurons in the superficial layers of V1 in anesthetized macaque monkeys, using microelectrode arrays. Spatial receptive fields were located in the lower visual field, at an eccentricity of 2-4 degrees. Recordings consisted of both well-isolated single units (13% of cases) and small multi-unit clusters that passed inclusion criteria (see Methods). Results for single- and multi-unit clusters were not distinguishable and are reported together.

We first measured responses to a drifting sinusoidal grating (target), alone and when paired with an overlapping, orthogonal grating (mask). These stimuli have been used extensively in previous work to measure masking in visual cortex (e.g., Morrone et al.,

1982; Bonds, 1989; DeAngelis et al., 1992; Carandini et al., 1997b,1998; Freeman et al., 2002). As expected, the mask reduced responses to target stimuli, particularly those of low contrast, as shown for an example unit in Figure 2A. To quantify the strength of masking, we computed a masking index, for which a value of 0 indicates no masking and a value of 1 indicates complete suppression of responses to the target (see Methods). For the example unit of Figure 2A, the masking index before adaptation was 0.15 for a 6% contrast mask, and 0.49 for a 50% mask. Across units, the average masking indices before adaptation were 0.21±0.01 (6% mask), 0.30±0.01 (12% mask), 0.38±0.02 (25% mask) and 0.58±0.01 (50% mask).

<Figure 2: Example cells>

We then tested the effect of contingent adaptation by consistently presenting the mask and target grating together (Figure 1B,C). For the example unit, contingent adaptation increased the suppressive influence of the mask; for the 25% contrast mask, the masking index increased from 0.33 to 0.55 after adaptation (compare the light and dark shaded areas in Figure 2A, top vs bottom). Across the population, contingent adaptation caused a consistent increase in the masking index. For the 25% contrast mask, the index increased by 0.21±0.02, or more than 50% (Figure 3A, green; $p<0.001$). With the exception of the lowest contrast mask, for which masking is weakest, contingent adaptation consistently strengthened the suppressive effect of the mask (Figure 3B, green; $p<0.001$ for 12%, 25% and 50% masks).

<Figure 3: Population results >

In stark contrast to the effects of contingent adaptation, asynchronous adaptation—interleaving the presentation of the target and mask—reduced masking. In the example unit of Figure 2B, the masking index for the 25% contrast mask was reduced from 0.39 before adaptation to 0 after adaptation. Across the population, the masking index for the 25% mask was reduced by 0.32±0.04, or nearly 85% (Figure 3A, blue). Similar effects

were evident for masks of other contrasts (Figure 3B, blue; $p<0.001$ for 6%, 25%, and 50% masks, $p=0.04$ for the 12% mask).

As evident for the example cells of Figure 2, both contingent and asynchronous adaptation also reduced responsivity to all stimuli. We consider the influence of altered responsivity on our measurements of masking below.

We tested the orientation specificity of adaptation-induced changes in masking by making separate measurements of masking with test stimuli that were rotated 45° relative to the adapters. Contingent adaptation weakened masking for rotated test stimuli on average, except for the highest contrast masks (Figure 3C,D, green; $p=0.09$ for 6%, $p=0.02$ for 12%, $p=0.05$ for 25%, and $p=0.64$ for 50% masks). Contingent adaptation's effect on masking strength was significantly affected by test stimulus orientation ($F(1,2096)=58.62$, $p<0.001$, ANOVA), with a significant interaction between mask contrast and stimulus orientation ($F(3,2096)=9.68$, $p<0.001$, ANOVA). Asynchronous adaptation weakened masking for rotated test stimuli, particularly at higher mask contrasts (Figure 3C,D, blue, $p=0.23$ for 6%, $p=0.38$ for 12%, and $p<0.001$ for 25% and 50% masks). The degree to which masking was weakened depended on whether test stimuli were matched in orientation to the adapters ($F(1,1236)=16.48$, $p<0.001$, ANOVA). There was no significant interaction between contrast and test stimulus orientation on the change in masking index ($F(3,1236)=1.03$, $p=0.38$, ANOVA).

In summary, the suppression recruited by a mask can be strengthened by consistently pairing the mask with a target (contingent adaptation), or weakened by interleaving its presentation with the target (asynchronous adaptation). These effects were orientation-specific: when test and adapting stimuli had different orientations, we saw less adaptation-induced change in masking. The orientation specificity of adaptation-induced changes in masking was consistent with similar orientation specificity for adaptation effects on contrast sensitivity (Sengpiel and Banhoeffer, 2002; Crowder et al., 2006; Dhruv et al., 2011) and orientation tuning (Müller et al., 1999; Dragoi et al., 2000; Patterson et al., 2013), and suggests a cortical contribution.

Dependence of adaptation effects on neuronal response properties

In the preceding analyses, we focused on average changes in masking across our entire sample. We now ask whether adaptation's effect on masking can be predicted by the functional properties of V1 neurons: their phase sensitivity (i.e., whether they are simple vs. complex), their orientation preference, and the properties of masking before adaptation.

Previous work has shown that the effects of adaptation may depend on whether neurons are simple or complex (Giaschi et al., 1993; but see Ohzawa et al., 1985 and Crowder et al., 2006), and that masking may be stronger in simple cells (Bonds, 1989). More critically, sensitivity to grating phase may influence measurements of masking, when cells are sensitive to both grating components. We thus tested for a relationship between a cell's phase sensitivity (the logarithm of the F1/F0 ratio; Skottun et al., 1991) and masking, both before and after adaptation. We found little relationship between the cell's phase sensitivity and the masking index before contingent (r=0.11, Spearman correlation; p=0.05) or asynchronous (r=0.04, p=0.53) adaptation in contrast to Bonds (1989). We also found no relationship between phase sensitivity and the change in masking after either contingent (r=-0.03, p=0.48) or asynchronous adaptation (r=0.06, p=0.39; Figure 4A). In cells with weak phase sensitivity (F0>F1), masking was stronger after contingent adaptation (increased by 0.24±0.03, p<0.001, n=217), and weaker after asynchronous adaptation (decreased by 0.38±0.03, p<0.001, n=140). In cells with strong phase sensitivity (F1>F0), masking was also stronger after contingent adaptation (increased by 0.13±0.05, p=0.02, n=100) and weaker after asynchronous adaptation (decreased by 0.16±0.09, p=0.07, n=53), though the latter effect was not statistically significant due likely to a smaller number of cells.

<Figure 4: Dependence of masking change on neuronal properties>

Previous studies have found that the effects of adaptation on V1 tuning depend on the relationship between the adapter and a neuron's stimulus preference (e.g., Dragoi et al., 2000; Crowder et al., 2006; Dhruv et al., 2011; Wissig and Kohn, 2012; Benucci et al.,

2013; Patterson et al., 2013). To assess whether adaptation-induced changes in masking depended on neuronal orientation preference, we recorded additional data in which we presented a reduced ensemble of test and mask gratings, interleaved with gratings of different orientations (see Methods).

We found that changes in masking were largely independent of neuronal orientation preference (Figure 4B). After contingent adaptation, masking was strengthened in cells whose preference was within 22.5° of either component of the plaid adapter (defined as 0° and 90°, thin black lines in Figure 4B), as well as in cells preferring orientations away from the plaid components (preferences offset by more than 22.5°). For the 50% mask, masking increased by 0.12±0.05 (p=0.007, n=53) and 0.31±-0.06 (p<0.001, n=62), respectively (p=0.02 for the comparison). Similarly, asynchronous adaptation led to weaker masking in cells with aligned (-0.18±0.07, p=0.03, n=47) and offset preferences (-0.22±0.07, p<0.001, n=65; p=0.69 for the comparison). We conclude that adaptation-induced changes in masking depend little, if at all, on neuronal orientation preference.

Our finding that changes in masking are evident in neurons with widely different preferences stands in contrast to the strong dependence of adaptation-induced changes in V1 tuning on preference, reported in previous studies. This divergence in outcome could reflect different specificity of adaptation-induced changes in masking and tuning. Alternatively, the different outcomes could arise because our masking experiments involved adapting with two orthogonal gratings, instead of single gratings as in previous work (Dragoi et al., 2000; Crowder et al., 2006; Dhruv et al., 2011; Wissig and Kohn, 2012; Patterson et al., 2013). To distinguish between these possibilities, we measured how changes in tuning gain depend on neuronal preference (see Methods), for contingent and asynchronous adapters. Gain was slightly weakened after contingent adaptation (Figure 4C, green), but this effect was indistinguishable in cells with well-aligned (geometric mean ratio of 0.92, p=0.003) and offset preferences (0.95, p=0.009; p=0.97 for comparison between groups). Similarly, asynchronous adaptation caused a decrease in tuning gain which was similar in cells with aligned and offset preferences (Figure 4C, blue; 0.61, p<0.001 vs 0.64, p<0.001; p=0.21 for comparison between

groups). Thus, changes in tuning curve gain are also broadly shared across neurons with different preferences.

Finally, we assessed whether the change in masking with adaptation depended on the strength of masking observed before adaptation. Specifically, we sought to determine whether the strengthening of masking after contingent adaptation was driven by cases in which the cross-oriented mask was facilitatory rather than suppressive (i.e., the pre-adaptation masking index less than 0). Carandini et al. (1998) reported that adaptation with plaids caused a specific reduction in V1 responsivity to plaids—which could contribute to an apparent increase in masking. The reduction in plaid responsivity in that study was particularly prevalent in neurons whose responses to targets were enhanced by the co-presentation of a mask (i.e., those that showed cross-orientation facilitation). In our data, masks were rarely facilitatory (5-15% of cases, depending on mask contrast). Further, we found that contingent adaptation strengthened masking, even after excluding units showing cross-orientation facilitation in control conditions (increase of 0.10±0.02, 0.17±0.02, and 0.05±0.02 for masks of 12, 25, and 50% contrast, respectively; $p<0.02$ for all cases; and decrease in masking of 0.08±0.02, $p<0.001$ for 6% masks). We conclude that the strengthening of masking after contingent adaptation cannot be attributed to a loss of cross-orientation facilitation, as in Carandini et al. (1998).

Controlling for adaptation-induced changes in responsivity

A notable consequence of both contingent and asynchronous adaptation is reduced neuronal responsivity. Since both adapters reduced responsivity, their opposite effects on masking cannot be trivially explained by altered responsivity. Additionally, adaptation's effect on responsivity (defined as the change in response to the high-contrast target after adaptation) was not related to the change in masking after contingent adaptation (Figure 5A; green, Spearman correlation of -0.06, p=0.26), and only weakly related to the change in masking after asynchronous adaptation (blue, r=0.18, p=0.01).

<Figure 5: Rate adaptation vs masking + rate match analysis>

The reduced responsivity after adaptation may nevertheless complicate inferences about how masking is altered by adaptation. For instance, adaptation might weaken masking because it fatigues the normalization pool rather than because it alters the interaction between the neuron and its normalization pool. We thus sought to determine how adaptation altered masking for stimuli of equal potency before and after adaptation.

To do so, we measured suppression through response summation. Specifically, we applied a 'rate-matched' suppression index, defined as:

$$SI = 1 - \frac{R_{TM}}{R_T + R_M}$$

where R_{TM} is the response to the full contrast plaid and R_T and R_M are the responses to the component gratings presented in isolation (Carandini et al., 1997b; Wissig and Kohn, 2012; Ruff et al., 2016). SI values near 0 indicate near-linear summation of responses to the component gratings (consistent with weak normalization); values near 1 indicate the response to the plaid is much weaker than expected from the responses to the component gratings (consistent with strong normalization).

We calculated the SI after adaptation using responses to the 50% contrast mask, the 50% contrast target, and the plaid made by their combination. We compared this SI to one measured before adaptation, obtained from target and mask gratings that generated responses equal to those observed for the 50% contrast gratings after adaptation (i.e., matched for response strength rather than for contrast; Figure 5B). Because the set of measured pre-adaptation responses rarely contained a perfect match to the post-adaptation responses, we fitted the pre-adaptation responses to a descriptive model and used the model to identify the necessary target and mask contrasts (see Methods). The model also allowed us to estimate responses to plaid stimuli composed of these rate-matched target and mask gratings. Thus, by comparing

573 the SI before and after adaptation we could test if adaptation alters response
574 summation (i.e., normalization), even for component gratings of matched potency.
575
576 Contingent adaptation caused the rate-matched SI to increase by 0.15±0.03 (p<0.001),
577 from an initial value of 0.06±0.03, a more than three-fold increase (Figure 5C, green;
578 n=58 units that passed selection criteria, see Methods). This increase is consistent with
579 a substantial strengthening of normalization. Asynchronous adaptation, conversely,
580 caused the SI to decrease by 0.36±0.08 (p<0.001) from an initial value of -0.13±0.03,
581 consistent with substantial weakening of normalization (Figure 5C, blue, n=51 units).
582 Note that pre-adaptation SI values were different for contingent and asynchronous
583 adapters (0.06 vs -0.13; p<0.001). This is because asynchronous adaptation reduced
584 responsivity more than contingent adaptation, so that the rate-matched pre-adaptation
585 responses were from lower contrasts for asynchronous adaptation. As masking is
586 weaker for low contrast stimuli, the pre-adaptation SI was lower in the asynchronous
587 adaptation condition.
588
589 For responses to rotated test stimuli, contingent adaptation caused no significant
590 change in SI (Figure 5D, green; -0.04±0.03 vs. 0.01±0.04; p=0.4). Asynchronous
591 adaptation caused a nearly two-fold reduction in SI (Figure 5D, blue; from -0.21±0.07 to
592 -0.43±0.08; p=0.003), consistent with a substantial weakening of normalization.
593
594 In summary, contingent adaptation caused responses to plaids to be even weaker than
595 expected from the linear sum of the component gratings, consistent with stronger
596 normalization; asynchronous adaptation, instead, caused summation to become more
597 linear, or even more supralinear, consistent with weaker normalization. Thus,
598 adaptation-induced changes in response summation are evident even for stimuli that
599 are equally potent before and after adaptation.
600
601 *Modeling adaptation's effect on normalization strength*
602 Westrick et al. (2016) proposed a specific learning rule for updating normalization
603 signals based on stimulus history. Their model posits that (1) the normalization signal

604 received by a target neuron arises from the response of a neuronal population, with the
605 response of each neuron in the pool receiving a distinct 'weight'; (2) the weights are
606 strengthened between the target neuron and the pool neurons that are consistently co-
607 activated, and weakened between those that are driven asynchronously (Figure 6A).
608 More precisely, the pairwise weight increases when the product of two neurons'
609 responses is greater than their homeostatic target, defined as their expected average
610 pairwise response (see Methods). Westrick et al. (2016) showed that the resultant
611 changes in normalization could capture a range of adaptation effects on tuning and
612 responsivity (Benucci et al., 2013). We therefore sought to determine whether this
613 model could also predict the adaptation-induced changes in masking that we observed.
614
615 <Figure 6: Model intuition>
616
617 The behavior of the model for contingent and asynchronous adaptation is illustrated in
618 Figure 6. During contingent adaptation, neurons that prefer orientations near 0° and 90°,
619 the orientations of the target and mask, will be strongly co-activated (Figure 6C, arrow,
620 lighter colors indicate stronger response products). Because the response product of
621 these neurons is larger than typical—that is, larger than their homeostatic target (Figure
622 6D, arrow)—the normalization weights for these neurons will be strengthened (Figure
623 6E, arrow, red indicates strengthening). Now consider neurons that prefer orientations
624 near 45°. The contingent adapter provides little drive to these neurons (Figure 6C, left,
625 white circle), so their response products are smaller than their homeostatic target.
626 Consequently, the normalization weights for these neurons weaken after contingent
627 adaptation (Figure 6E, blue). Note that the manner in which the normalization weights
628 change after adaptation is not equivalent to that predicted by the initial response
629 product. The change depends also on the homeostatic target; further, as the
630 normalization weights adjust, the neurons' responses evolve as well.
631
632 The effect of asynchronous adaptation can be understood similarly. These adapters
633 provide strong drive to neurons preferring orientations near 0 and 90°, but the two sets
634 of neurons are active at different phases of the adapter (Figure 6G). Thus, normalization

weights are strengthened for pairs responding to either 0 or 90° orientations, but weakened between 0-90° pairs (Figure 6I).

Both contingent and asynchronous adaptation strengthen some normalization weights and weaken others, but the pattern of weight changes across the population of units differs between adapters, resulting in different effects on masking. For a neuron whose preference is matched to the target (0°), masking is strengthened after contingent adaptation (Figure 6F), compared to the masking evident before adaptation (Figure 6B). There is more masking because the weights between neurons preferring 0° (the target) and 90° are strengthened, resulting in greater suppression. After asynchronous adaptation, these same weights are weakened, resulting in less masking (Figure 6J). In addition, asynchronous adaptation strengthens weights between neurons whose preferences are near 0°, resulting in weaker responses to the target itself (Figure 6J). Note that this change in responsivity—also evident in our neurophysiological data—arises solely from altered normalization, as the model contains no other mechanism for adjusting to prolonged sensory input.

<Figure 7: Model results>

Across the population of units, the model predicts that contingent adaptation should strengthen masking (Figure 7A, green, dashed line), particularly for higher mask contrasts, as in the neuronal data. Asynchronous adaptation leads to weakened masking (Figure 7A, blue, dashed line). However, this instantiation of the model underestimates the magnitude of altered masking in the data. Further, although changes in masking in the model depend on whether the test stimuli are matched to the adapter (compare dashed lines in Figure 7A and Figure 7B, which illustrates changes in masking for test stimuli offset by 45° from the adapter), the predicted effects are different from those we observed. Finally, the model predicts that the degree to which masking is altered by adaptation depends strongly on neuronal preference (dashed lines in Figure 7C,D), which was not the case in our data.

The behavior of the model depends critically on several parameters, including the tuning widths of the units (which may or may not be equivalent to V1 tuning, depending on the source of normalization), the time scale of the model, the contrast saturation of the model neurons, and the training contrast, which determines the homeostatic response target for each pair. For many parameter settings that produced stronger changes in normalization, the model tends to predict unrealistic response facilitation in units whose normalization signals are weakened. We therefore considered a simple extension to the model to mitigate this behavior (see Methods): a 'fatigue' mechanism that reduces responsivity in proportion to recent activity levels, as described in previous neurophysiological studies (Schwindt et al., 1988; Sanchez-Vives, 2000a, 2000b; see Carandini and Ferster, 1997 for related work). With this mechanism, the model was able to produce changes in masking similar to those in our data (Figure 7A, solid lines), including the dependence on test stimulus orientation (Figure 7B, solid lines), with limited response facilitation for moderate contrast stimuli. However, this model still incorrectly predicts that changes in masking depend on neuronal preference (Figure 7C,D; solid lines).

In summary, a simple learning rule for updating normalization weights—developed to account for an entirely distinct set of adaptation phenomena—qualitatively matched many of our key physiological observations: opposite changes in masking after contingent and asynchronous adaptation; and a dependence of the changes in masking on stimulus contrast and the relative orientation of the adapters and test stimuli; and stronger loss of responsivity after asynchronous than contingent adaptation;. An unresolved mismatch with the data is the model's prediction that changes in masking depend strongly on neuronal preference. One explanation for this discrepancy is that the V1 neurons with offset preferences for which we measured masking all had appreciable responses to the target grating—a requirement for measured masking. As a result, these cells were well driven by the adapter and might be predicted to show stronger masking after adaptation. In the model, masking can be measured for arbitrarily small responses; thus, the change in masking for units with offset preferences includes poorly driven units. We note that the model might be made to better fit our data

(e.g., through a more exhaustive search of parameters), but such a data-fitting exercise would only be meaningful if it were constrained by a broader set of adaptation phenomena, including those used to develop the original model.

DISCUSSION

We found that masking is enhanced when a mask and target grating are consistently paired, but weakened when those stimuli are presented asynchronously. Changes in masking depend on the orientation of the stimulus relative to the orientation of the adapter, but are shared broadly across the population, independent of neuronal preference. Altered masking cannot be attributed to weaker stimulus potency after adaptation, or to changes in neuronal responsivity. Our results thus show that a paradigmatic form of normalization in visual cortex can be either strengthened or weakened, depending on the temporal contingencies between different visual inputs.

Relation to previous work

Previous reports have provided conflicting evidence for adaptation's effect on masking. Freeman et al. (2002) found no change in masking in cat V1 after adaptation with the mask grating. Li et al. (2005) found that dichoptic but not monoptic masking was reduced by adaptation. The authors concluded that there are two mechanisms of masking: one subcortical, monocular, and unadaptable; the other cortical, binocular, and adaptable. It is unclear why the cortical mechanism was not evident in their monocular adaptation experiments, but the adaptable mechanism of masking they identified might underlie the weakened masking we observe after asynchronous adaptation. In related work, Dhruv et al. (2011) measured the effects of adaptation in macaque V1. After adaptation with orthogonally-oriented gratings, responses to high-contrast preferred stimuli were often elevated. By fitting a descriptive model to their data, the authors inferred that this facilitation was due to weakened normalization after adaptation, consistent with our measurements with asynchronous adapters. Previous evidence that adaptation can strengthen masking is scant. In a brief report, Carandini et al. (1998) measured the effect of adapting to plaids or gratings in 8 cat V1 cells. They showed that adaptation altered cross-orientation interactions in 5 of these cells,

728 including weakening of cross-orientation facilitation and strengthening of suppression.
729 These observation are consistent with our more extensive and systematic observations,
730 although we found little role for reduced cross-orientation facilitation in our results.
731
732 Our finding that masking can be strongly influenced by adaptation is consistent with
733 recent reports that surround suppression—another form of normalization (Heeger, 1992;
734 Cavanaugh et al., 2002; Carandini and Heeger, 2012; Coen-Cagli et al., 2012, 2015)—
735 can be altered by adaptation (Webb et al., 2005; Camp et al., 2009; Patterson et al.,
736 2014). Specifically, these studies showed that adaptation with an annular grating, a form
737 of asynchronous adaptation in which the surround but not the center receives visual
738 input, leads to weaker suppression. However, it has also been shown that adapting with
739 large gratings—which should provide 'contingent' co-activation of the receptive field and
740 its surround—can lead to response facilitation (Wissig and Kohn, 2012; Patterson et al.,
741 2013, 2014), implying weaker suppression. This may indicate that there are distinct
742 rules by which suppressive signals within the receptive field and from the surround are
743 updated by adaptation, consistent with their having distinct underlying mechanisms
744 (Sengpiel et al., 1998). Alternatively, adaptation with large gratings may potentiate the
745 suppression of normalization signals within the receptive field by the surround (i.e., a
746 stronger suppression of suppression, leading to facilitation; Trott and Born, 2015).
747
748 Stronger masking was evident after the contingent display of the mask and target.
749 Numerous perceptual studies have also reported contingent adaptation effects. Perhaps
750 the most well-known is the 'McCollough effect' in which adaptation to colored, oriented
751 gratings induces an orientation-dependent color aftereffect (McCollough, 1965; see also
752 Hepler, 1968; Held and Shattuck, 1971; Favreau et al., 1972; Lovegrove and Over,
753 1972). The large number of possible stimulus contingencies makes it unlikely that these
754 perceptual effects arise from the fatigue of cells selective for each pairing. Instead, they
755 could be explained by altered interactions between neurons selective for different
756 stimulus features (Barlow and Földiák, 1989; Barlow, 1990).
757
758 <Figure 8: Recovery>

The attribution of contingent perceptual aftereffects to altered neuronal interactions is similar in spirit to the altered normalization suggested by our masking experiments, since normalization is likely a network phenomenon. However, it is unlikely our observations underlie the types of perceptual contingent aftereffects cited above. First, most of the perceptual effects persist for many hours, even after relatively brief (tens of seconds) adaptation (McCollough, 1965; Vul et al., 2008). The changes in masking we observe are more transient, as shown in Figure 8: the effects of contingent (green) and asynchronous (blue) adaptation entirely dissipated after a 10-15 minute recovery period. Second, the perceptual experiments involve a single adapter (consisting of paired stimuli) which induces distinct aftereffects depending on the test stimulus. We show, instead, distinct changes in masking with different adapters using a single ensemble of test stimuli.

Although our results are unlikely to underlie classic contingent aftereffects, our findings do have a direct perceptual correlate in human observers: contingent adaptation leads to greater perceptual masking, whereas asynchronous adaptation leads to weaker masking (Yiltiz et al., 2018; see also Foley and Chen, 1997).

Mechanisms

The biophysical and circuit mechanisms underlying masking within the RF (i.e., cross-orientation suppression) are not fully understood. Some have suggested that masking involves depression of thalamocortical synapses (Carandini et al., 2002; Freeman et al., 2002; but see Li et al., 2006). Others have suggested that masking arises from rectification and weak contrast saturation in LGN responses (Li et al., 2006), perhaps amplified by a non-linear input-output transformation in cortex (Priebe and Ferster, 2006).

The changes in masking we observe during adaptation are difficult to reconcile with any of these proposed mechanisms. Both contingent and asynchronous adapters should recruit robust responses in the LGN (Priebe and Ferster, 2006) and thus depress

790 thalamocortical synapses. In this adapted state, presenting a target and mask together
791 would likely produce little additional depression (Boudreau and Ferster, 2005; Reig et
792 al., 2006). Thus, synaptic-depression models may predict weaker masking after
793 adaptation but cannot account for stronger masking after contingent adaptation. If,
794 instead, cortical masking is largely inherited from the LGN, our results would require
795 that geniculate neurons adapt differently to contingent and asynchronous adapters.
796 However, neurons in cat and monkey LGN adapt weakly (Movshon and Lennie, 1979;
797 Ohzawa et al., 1985; Nelson, 1991; Sanchez-Vives et al., 2000a; but see Shou et al.,
798 1996 and Duong and Freeman, 2007) except when driven by stimuli of much higher
799 temporal frequency than those we used (Solomon et al., 2004). In addition, adaptation
800 effects in the LGN show no evidence of the orientation specificity we observe for altered
801 masking (Solomon et al., 2004).
802
803 Our results are qualitatively consistent with a recently-proposed rule for updating
804 normalization weights based on stimulus history (Westrick et al., 2016; see also related
805 work by Hosoya et al., 2005). The model correctly predicts that masking is strengthened
806 by contingent adaptation and weakened by asynchronous adaptation. It captures these
807 effects solely through modulating the normalization weights between units with different
808 tuning, based on their degree of co-activation during adaptation. Because the model's
809 behavior only depends on the pattern of response co-activation, it could also be used to
810 predict changes in normalization for more complex stimuli (e.g., natural scenes), if
811 based on receptive field models that accurately capture responses to those stimuli.
812
813 Although the mechanisms responsible for masking remain unclear, our finding that
814 changes in masking depend on the temporal relationship between adapters suggests a
815 Hebbian-like mechanism is responsible for their updating (Westrick et al., 2016). There
816 is, of course, extensive evidence for Hebbian plasticity of synaptic strength, on a range
817 of time scales (Abbott and Regehr, 2004; Abbott and Nelson, 2000). Masking may thus
818 be modified by the synaptic plasticity between target neurons and those neurons
819 providing suppressive input. This synaptic plasticity could involve changes in inhibitory

820 synapses, or a more complex rebalancing of excitatory and inhibitory input (Sato et al.,
821 2016; Nassi et al., 2015; Rubin et al., 2015).
822
823 We note that the masking we measured was driven primarily by suppressive signals
824 within the RF, because we used small stimuli (1.5° diameter) centered on the aggregate
825 RF of the recorded units. However, the size of our stimuli was slightly larger than the
826 average spatial RF of V1 neurons at the targeted eccentricity (Cavanaugh et al., 2002).
827 As a result, our stimuli may have recruited some surround suppression. However, as
828 noted above, surround signals are modified by adaptation in a manner seemingly
829 distinct from the effects we report here. Thus, it is unlikely that the adaptation-induced
830 changes in masking involved altered suppression from the RF surround.
831
832 *Implications*
833 Our results have several important implications for our understanding of normalization
834 and of adaptation.
835
836 Although initially developed to account for non-linear response properties of V1
837 neurons, normalization has now been shown to be useful for explaining a broad set of
838 phenomena (Carandini and Heeger, 2012). Across these contexts, normalization is
839 often portrayed as a largely static computation, although recent work has shown that
840 attention may modulate normalization signals dynamically (Lee and Maunsell, 2009;
841 Reynolds and Heeger, 2009). Our results, and those on adaptation effects in the
842 surround, indicate that normalization can also be modulated dynamically based on
843 recent sensory input (Solomon and Kohn, 2014). In so far as our results are consistent
844 with the updating rule of Westrick et al. (2016), our results also provide an indication as
845 to how the set-point of normalization signals may be calibrated to match the dominant
846 statistics of the sensory environment.
847
848 Normalization is thought to be critical for a number of inter-related cortical functions,
849 including improving representational efficiency (Schwartz and Simoncelli, 2001; Coen-
850 Cagli et al., 2012); performing marginalization, a basic computation in probabilistic

inference (Beck et al., 2011); implementing predictive coding (Spratling, 2010; Lochmann et al., 2012); and determining stimulus salience (Itti and Koch, 2000). Because normalization signals are strongly shaped by adaptation, a primary purpose of adaptation effects may be to modulate these computations. For instance, changes in neuronal tuning and responsivity may maintain or improve representational efficiency (Barlow and Földiák, 1989; Barlow, 1990; Wainwright et al., 2002) or highlight novel features of the environment (Hosoya et al., 2005; Solomon and Kohn, 2014). Alternative hypotheses of the functional benefits of adaptation would need to account for the strong modulation of normalization that occurs with adaptation.

Our finding that the updating of normalization-based suppressive signals is sensitive to temporal contingencies between visual inputs offers cortical networks the ability to adjust not only to the persistence or frequency of occurrence of individual stimuli, but also to the relationships among stimuli. Neurons in higher visual cortex are known to become sensitive to temporal (sequential) pairings of stimuli through learning that occurs over weeks (Meyer and Olson, 2011). Our results show that sensitivity to temporal relationships among stimuli can emerge after much briefer exposures, even in the earliest stages of cortical visual processing.

Finally, our findings lend credence to frameworks in which adaptation effects arise, in part, from altered normalization (Heeger, 1992; Wainwright et al., 2002; Lochmann et al., 2012; Solomon and Kohn, 2014; Snow et al., 2016; Westrick et al., 2016). While such frameworks have been shown to account for a broad set of adaptation phenomena, their key assumption—that adaptation alters normalization—has received limited experimental support, except for demonstrations that surround suppression can be weakened by adaptation. Our finding that normalization can be robustly strengthened or weakened opens the door to the development of a normalization-based framework for understanding adaptation. Such a framework might be able to predict effects for a much broader set of adaptation paradigms than usually considered (e.g., natural scenes, natural viewing), as well as offering new mechanistic, network-based explanations for how cortex adjusts to current sensory demands.

882

883

884 **REFERENCES**

885 Abbott LF, Nelson SB (2000) Synaptic plasticity: taming the beast. Nature Neuroscience
886 3:1178-1183.
887 Abbott LF, Regehr WG (2004) Synaptic computation. Nature 431: 796-803.
888 Barlow HB, Földiák P (1989) Adaptation and decorrelation in the cortex. In: The
889 computing neuron (Durbin R, Miall C, Mitchinson G, eds), pp 54 – 72. New York:
890 Addison-Wesley.
891 Barlow HB (1990) A theory about the functional role and synaptic mechanism of visual
892 after-effects. In Vision: Coding and efficiency (Blakemore CB, ed), pp 363-375.
893 New York: Cambridge University Press.
894 Beck JM, Latham PE, Pouget A (2011) Marginalization in neural circuits with divisive
895 normalization. Journal of Neuroscience 31:15310-15319.
896 Benucci A, Saleem AB, Carandini M (2013) Adaptation maintains population
897 homeostasis in primary visual cortex. Nature Neuroscience 16:724-729.
898 Bonds AB (1989) Role of inhibition in the specification of orientation selectivity of cells in
899 the cat striate cortex. Visual Neuroscience 2:41-55.
900 Boudreau CE, Ferster D (2005). Short-term depression in thalamocortical synapses of
901 cat primary visual cortex. Journal of Neuroscience 25:7179-7190.
902 Camp AJ, Tailby C, Solomon SG (2009) Adaptable mechanisms that regulate the
903 contrast response of neurons in the primate lateral geniculate nucleus. Journal of
904 Neuroscience 29:5009-5021.
905 Carandini M, Heeger DJ, Movshon JA (1997a) Linearity and normalization in simple
906 cells of the macaque primary visual cortex. Journal of Neuroscience 17:8621-8644.
907 Carandini M, Barlow HB, O'Keefe LP, Poirson AB, Movshon JA (1997b). Adaptation to
908 contingencies in macaque primary visual cortex. Philosophical Transactions of the
909 Royal Society of London B: Biological Sciences 352:1149-1154.
910 Carandini M, Ferster D (1997c) A tonic hyperpolarization underlying contrast adaptation
911 in cat visual cortex. Science 276:949-952.
912 Carandini M, Movshon JA, Ferster D (1998) Pattern adaptation and cross-orientation
913 interactions in the primary visual cortex. Neuropharmacology 37:501-511.

914 Carandini M, Heeger DJ, Senn W (2002) A synaptic explanation of suppression in visual
915 cortex. Journal of Neuroscience 22:10053-10065.
916 Carandini M, Heeger DJ (2012) Normalization as a canonical neural computation.
917 Nature Reviews Neuroscience 13:51-62.
918 Cavanaugh JR, Bair W, Movshon JA (2002) Nature and interaction of signals from the
919 receptive field center and surround in macaque V1 neurons. Journal of
920 Neurophysiology 88:2530-2546.
921 Clifford CW, Webster MA, Stanley GB, Stocker AA, Kohn A, Sharpee TO, Schwartz O
922 (2007) Visual adaptation: Neural, psychological and computational aspects. Vision
923 Research 47:3125-3131.
924 Coen-Cagli R, Dayan P, Schwartz O (2012) Cortical surround interactions and
925 perceptual salience via natural scene statistics. PLoS Computational Biology, 8,
926 e1002405.
927 Coen-Cagli R, Kohn A, Schwartz O (2015) Flexible gating of contextual influences in
928 natural vision. Nature Neuroscience 18:1648.
929 Crowder NA, Price NS, Hietanen MA, Dreher B, Clifford CW, Ibbotson MR (2006)
930 Relationship between contrast adaptation and orientation tuning in V1 and V2 of
931 cat visual cortex. Journal of Neurophysiology 95:271-283.
932 DeAngelis GC, Robson JG, Ohzawa I, Freeman RD (1992) Organization of suppression
933 in receptive fields of neurons in cat visual cortex. Journal of Neurophysiology
934 68:144-163.
935 Dhruv NT, Tailby C, Sokol SH, Lennie P (2011) Multiple adaptable mechanisms early in
936 the primate visual pathway. Journal of Neuroscience 31:15016-15025.
937 Dragoi V, Sharma J, Sur M (2000) Adaptation-induced plasticity of orientation tuning in
938 adult visual cortex. Neuron 28:287-298.
939 Duong T, Freeman RD (2007) Spatial frequency-specific contrast adaptation originates
940 in the primary visual cortex. Journal of Neurophysiology 98:187-195.
941 El-Shamayleh Y, Movshon JA (2011) Neuronal responses to texture-defined form in
942 macaque visual area V2. The Journal of Neuroscience 31:8543-8555.
943 Favreau OE, Emerson VF, Corballis MC (1972) Motion perception: A color-contingent
944 aftereffect. Science 176:78-79.

945 Foley JM, Chen CC (1997) Analysis of the effect of pattern adaptation on pattern
946 pedestal effects: a two-process model. Vision Research 37:2779-2788.
947 Freeman TC, Durand S, Kiper DC, Carandini M (2002) Suppression without inhibition in
948 visual cortex. Neuron 35:759-771.
949 Giaschi D, Douglas R, Marlin S, Cynader M (1993) The time course of direction-
950 selective adaptation in simple and complex cells in cat striate cortex. Journal of
951 Neurophysiology 70:2024-2034.
952 Heeger DJ (1992) Normalization of cell responses in cat striate cortex. Visual
953 Neuroscience 9:181-197.
954 Held R, Shattuck SR (1971) Color-and edge-sensitive channels in the human visual
955 system: Tuning for orientation. Science 174:314-316.
956 Hepler N (1968) Color: A motion-contingent aftereffect. Science 162:376-377.
957 Hosoya T, Baccus SA, Meister M (2005) Dynamic predictive coding by the retina.
958 Nature 436:71-77.
959 Itti L, Koch C (2000) A saliency-based search mechanism for overt and covert shifts of
960 visual attention. Vision Research 40:1489-1506.
961 Kaliukhovich DA, Vogels R (2016) Divisive normalization predicts adaptation-induced
962 response changes in macaque inferior temporal cortex. Journal of Neuroscience
963 36:6116-6128.
964 Kelly RC, Smith MA, Samonds JM, Kohn A, Bonds AB, Movshon JA, Lee TS (2007)
965 Comparison of recordings from microelectrode arrays and single electrodes in the
966 visual cortex. Journal of Neuroscience 27:261-264.
967 Kohn A (2007) Visual adaptation: physiology, mechanisms, and functional benefits.
968 Journal of Neurophysiology 97:3155-3164.
969 Kohn A, Movshon JA (2004) Adaptation changes the direction tuning of macaque MT
970 neurons. Nature Neuroscience 7:764-772.
971 Lee J, Maunsell JH (2009) A normalization model of attentional modulation of single unit
972 responses. PLoS One 4:e4651.
973 Li B, Peterson MR, Thompson JK, Duong T, Freeman RD (2005) Cross-orientation
974 suppression: monoptic and dichoptic mechanisms are different. Journal of
975 Neurophysiology 94:1645-1650.

Li B, Thompson JK, Duong T, Peterson MR, Freeman RD (2006) Origins of cross-orientation suppression in the visual cortex. Journal of Neurophysiology 96:1755-1764.

Lochmann T, Ernst UA, Deneve S (2012) Perceptual inference predicts contextual modulations of sensory responses. Journal of Neuroscience 32:4179-4195.

Lovegrove WJ, Over R (1972) Color adaptation of spatial frequency detectors in the human visual system. Science 176:541-543.

McCollough C (1965) Color adaptation of edge-detectors in the human visual system. Science, 149, 1115-1116.

Meyer T, Olson CR (2011) Statistical learning of visual transitions in monkey inferotemporal cortex. Proceedings of the National Academy of Sciences 108:19401-19406.

Morrone MC, Burr DC, Maffei L (1982) Functional implications of cross-orientation inhibition of cortical visual cells. I. Neurophysiological evidence. Proceedings of the Royal Society of London B: Biological Sciences 216:335-354.

Movshon JA, Lennie P (1979) Pattern-selective adaptation in visual cortical neurones. Nature 278:850.

Müller JR, Metha AB, Krauskopf J, Lennie P (1999) Rapid adaptation in visual cortex to the structure of images. Science 285:1405-1408.

Nassi JJ, Avery MC, Cetin AH, Roe AW, Reynolds JH (2015) Optogenetic Activation of Normalization in Alert Macaque Visual Cortex. Neuron 86: 1504-1517.

Nelson SB (1991) Temporal interactions in the cat visual system. I. Orientation-selective suppression in the visual cortex. Journal of Neuroscience 11:344-356.

Ohzawa I, Sclar G, Freeman RD (1985) Contrast gain control in the cat's visual system. Journal of Neurophysiology 54:651-667.

Patterson CA, Wissig SC, Kohn A (2013) Distinct effects of brief and prolonged adaptation on orientation tuning in primary visual cortex. Journal of Neuroscience 33:532-543.

Patterson CA, Duijnhouwer J, Wissig SC, Krekelberg B, Kohn A (2014) Similar adaptation effects in primary visual cortex and area MT of the macaque monkey under matched stimulus conditions. Journal of Neurophysiology, 111: 1203-1213.

1007 Priebe NJ, Ferster D (2006) Mechanisms underlying cross-orientation suppression in
1008 cat visual cortex. Nature Neuroscience 9:552-561.
1009 Reig R, Gallego R, Nowak LG, Sanchez-Vives MV (2006) Impact of cortical network
1010 activity on short-term synaptic depression. Cerebral Cortex 16:688-695.
1011 Rieke F, Rudd ME (2009) The challenges natural images pose for visual adaptation.
1012 Neuron 64:605-616.
1013 Reynolds JH, Heeger DJ (2009) The normalization model of attention. Neuron 61:168-
1014 185.
1015 Rubin DB, Van Hooser SD, Miller KD (2015) The stabilized supralinear network: a
1016 unifying circuit motif underlying multi-input integration in sensory cortex. Neuron.
1017 85: 402-417
1018 Ruff DA, Alberts JJ, Cohen MR (2016) Relating normalization to neuronal populations
1019 across cortical areas. Journal of Neurophysiology 116:1375-1386.
1020 Sanchez-Vives MV, Nowak LG, McCormick DA (2000a) Membrane mechanisms
1021 underlying contrast adaptation in cat area 17 in vivo. Journal of Neuroscience
1022 20:4267-4285.
1023 Sanchez-Vives MV, Nowak LG, McCormick DA (2000b) Cellular mechanisms of long-
1024 lasting adaptation in visual cortical neurons in vitro. Journal of Neuroscience
1025 20:4286-4299.
1026 Sato TK, Haider B, Häusser M, Carandini M (2016) An excitatory basis for divisive
1027 normalization in visual cortex. Nature Neuroscience 19: 568-570.
1028 Schwartz O, Hsu A, Dayan P (2007) Space and time in visual context. Nature Reviews
1029 Neuroscience 8:522-535.
1030 Schwartz O, Simoncelli EP (2001) Natural signal statistics and sensory gain control.
1031 Nature Neuroscience 4:819-825.
1032 Schwindt PC, Spain WJ, Foehring RC, Chubb MC, Crill WE (1988) Slow conductances
1033 in neurons from cat sensorimotor cortex in vitro and their role in slow excitability
1034 changes. Journal of Neurophysiology 59:450-467.
1035 Sengpiel F, Bonhoeffer T (2002) Orientation specificity of contrast adaptation in visual
1036 cortical pinwheel centres and iso-orientation domains. European Journal of
1037 Neuroscience 15:876-886.

1038 Sengpiel F, Baddeley RJ, Freeman TC, Harrad R, Blakemore C (1998) Different
1039 mechanisms underlie three inhibitory phenomena in cat area 17. Vision Research
1040 38:2067-2080.
1041 Shou T, Li X, Zhou Y, Hu B (1996) Adaptation of visually evoked responses of relay
1042 cells in the dorsal lateral geniculate nucleus of the cat following prolonged
1043 exposure to drifting gratings. Visual Neuroscience 13:605-613.
1044 Skottun BC, De Valois RL, Grosof DH, Movshon JA, Albrecht DG, Bonds AB (1991)
1045 Classifying simple and complex cells on the basis of response modulation. Vision
1046 Research 31:1079-1086
1047 Snow M, Coen-Cagli R, Schwartz O (2016) Specificity and timescales of cortical
1048 adaptation as inferences about natural movie statistics. Journal of Vision 16(13):1.
1049 Solomon SG, Peirce JW, Dhruv NT, Lennie P (2004) Profound contrast adaptation early
1050 in the visual pathway. Neuron 42:155-162.
1051 Solomon SG, Kohn A (2014) Moving sensory adaptation beyond suppressive effects in
1052 single neurons. Current Biology 24:R1012-R1022.
1053 Spratling MW (2010) Predictive coding as a model of response properties in cortical
1054 area V1. Journal of Neuroscience 30:3531-3543.
1055 Stocker AA, Simoncelli EP (2006) Noise characteristics and prior expectations in human
1056 visual speed perception. Nature Neuroscience 9:578-585.
1057 Trott AR, Born RT (2015) Input-gain control produces feature-specific surround
1058 suppression. Journal of Neuroscience 35:4973-4982.
1059 Vul E, Krizay E, MacLeod DI (2008) The McCollough effect reflects permanent and
1060 transient adaptation in early visual cortex. Journal of Vision 8(12):4.
1061 Wainwright MJ, Schwartz O, Simoncelli EP (2002) Natural image statistics and divisive
1062 normalization: Modeling nonlinearity and adaptation in cortical neurons. In:
1063 Probabilistic models of the brain: Perception and neural function (Rao RPN,
1064 Olshausen BA, Lewicki MS, eds), pp 203-222. Cambridge, Mass.: MIT Press.
1065 Wark B, Lundstrom BN, Fairhall A (2007) Sensory adaptation. Current Opinion in
1066 Neurobiology 17:423-429.

1067 Webb BS, Dhruv NT, Solomon SG, Tailby C, Lennie P (2005) Early and late
1068 mechanisms of surround suppression in striate cortex of macaque. Journal of
1069 Neuroscience 25:11666-11675.
1070 Webster MA (2015) Visual adaptation. Annual Review of Vision Science 1:547-567.
1071 Westrick ZM, Heeger DJ, Landy MS (2016) Pattern adaptation and normalization
1072 reweighting. Journal of Neuroscience 36:9805-9816.
1073 Wissig SC, Kohn A (2012) The influence of surround suppression on adaptation effects
1074 in primary visual cortex. Journal of Neurophysiology 107:3370-3384.
1075 Yiltiz H, Heeger DJ, Landy MS (2018) Contingent adaptation in masking and surround
1076 suppression. Journal of Vision, forthcoming abstract.
1077

FIGURE LEGENDS

Figure 1. Stimulus protocol. (**A**) The ensemble of test stimuli ("T"). (**B**) The temporal structure and form of the contingent and asynchronous adapters ("A"). (**C**) The temporal structure of the experiment, which involved measuring responses before adaptation, adapting, and then measuring responses using a top-up/test paradigm.

Figure 2. Example neurons (**A**) Example unit for contingent adaptation. (Top) Contrast-response functions for target stimuli presented in isolation or with masks of different contrasts (indicated by symbols with different shades of gray). Responses are measured relative to the response evoked by each mask. Fill indicates the area-under-the-curve, used to calculate the masking index. Position of the symbols along the abscissa have been jittered slightly to improve visibility. (Bottom) Responses of the same cell after contingent adaptation. (**B**) Example unit for asynchronous adaptation, following the conventions of (**A**). The error bars show 1 SEM.

Figure 3. Population summary. (**A**) Change in masking index for the 25% contrast mask (post-adaptation values minus pre-adaptation values) when test stimuli are matched in orientation to the adapter. Data for contingent adaptation are shown in green; for asynchronous adaptation, in blue. Values larger than zero indicate stronger masking; less than zero indicates weaker masking. Arrowheads indicate mean of the distributions. (**B**) Mean change in masking index after contingent (green) or asynchronous (blue) adaptation, as a function of mask contrast. (**C,D**) Effects of contingent and asynchronous adaptation on test stimuli whose orientation is rotated by 45° from the adapter, following the conventions of (**A,B**). The error bars show 1 SEM.

Figure 4. Dependence of changes in masking on neuronal properties. (**A**) Relationship between adaptation-induced changes in masking index and phase sensitivity, as measured by the F1/F0 response ratio. Each dot represents effects for 25% contrast masks for one unit. (**B**) Relationship between adaptation-induced changes in masking index and each neuron's orientation preference, where 0° and 90° indicate

preferences aligned with the component gratings (indicated by vertical thin black lines). (**C**) Relationship between adaptation induced changes in tuning gain and each neuron's orientation preference, following the conventions of (**B**).

Figure 5. Controlling for rate adaptation. (**A**) The relationship between the change in masking index and responsivity change, measured as the ratio of response to the high contrast target after vs. before adaptation. Masking was measured using 25% contrast masks. Each dot indicates one unit. (**B**) Method for calculating rate-matched suppression index (SI). Filled symbols in the right panel indicate the measured responses to the 50% contrast target (black), the 50% contrast mask (cyan), and the plaid formed by their combination (yellow). Filled symbols in the left panel indicate the target and mask contrasts that evoked matched responses (indicated by dashed horizontal lines), and the plaid formed by their combination. (**C**) Histogram of the change in rate-matched SI after contingent (green) and asynchronous (blue) adaptation. Arrowheads indicate distribution mean. (**D**) Histogram of the change in rate-matched SI for test stimuli whose orientation was rotated by 45° from the adapters. Conventions as in (**C**).

Figure 6. Hebbian normalization model. (**A**) Schematic of the normalization model and the learning rule (see Westrick et al., 2016). The normalization signal received by each neuron arises from the weighted responses of other neurons in the population. The weights between neurons that are consistently co-activated (white triangles) are strengthened (red dots), whereas the weights are weakened between neurons that are driven asynchronously (blue dots). (**B**) Simulated contrast-response function before adaptation to the target alone (light gray) and the target presented with a 50% mask (dark gray) for a neuron preferring the orientation of the target grating. (**C**) Response products to the plaid contingent adapter. Lighter color indicates stronger response products. Arrow indicates neuron-pair preferring 0 and 90°. Circle indicates neuron-pair preferring 45°. (**D**) The homeostatic target defined as the average response products to a uniform distribution of oriented gratings. Markers indicate the same neuron pairs as **C.** (**E**) Change in normalization weights after contingent adaptation. Markers indicate the

same pairs as **C**. (**F**) Contrast response function after contingent adaptation in the same convention as **B**. (**G-J**) Same conventions as **C-F** after asynchronous adaptation.

Figure 7. Model predictions for changes in masking after contingent or asynchronous adaptation. (**A**) (Left) Changes in masking index in simulated neurons, as a function of mask contrast, after contingent (green) and asynchronous (blue) adaptation for test stimuli matched in orientation to the adapters. Dotted lines indicate mean of simulated population of model neurons, averaged across all orientation preferences. Solid lines indicate mean of simulated population of neurons from the extended model (i.e., with a fatigue mechanism). Shading indicates standard deviation across model neurons with different orientation preferences. (**B**) Same as **A** for test stimuli offset in orientation from the adapters. Dashed curve for asynchronous adaptation has been scaled slightly for visualization. (**C**) Change in masking index for the 50% contrast mask, as a function of model unit orientation preference, for test stimuli matched in orientation to the adapter. (**D**) Same as **C** for test stimuli offset in orientation from the adapters. Dashed curve for asynchronous adaptation has been scaled slightly for visualization.

Figure 8. Recovery from adaptation. The average masking index for the 25% contrast mask before adaptation, after contingent (green) or asynchronous (blue) adaptation, and 10-15 minutes later, after the continuous presentation of a gray screen. Adaptation-induced changes in masking dissipated entirely during the recovery period; in fact, they often showed a slight rebound effect, with masking in the recovery period slightly weaker (stronger) than the pre-adaptation measurements for contingent (asynchronous) adaptation. The error bars show 1 SEM. Contingent and asynchronous lines were separated by which adaptation paradigm was recorded first (both were always run back-to-back). Units shown are a subset of the full data set, representing neurons whose isolation was stable throughout the recovery period.

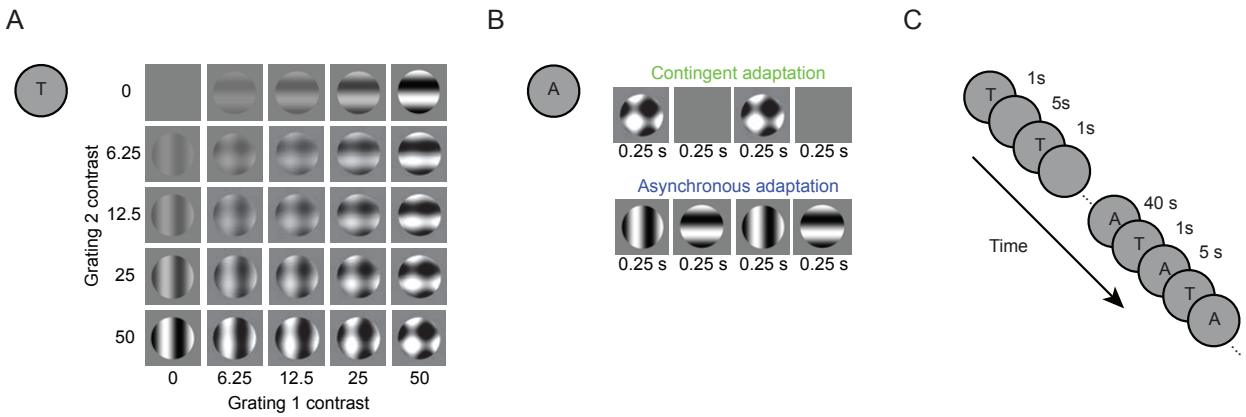

Figure 1

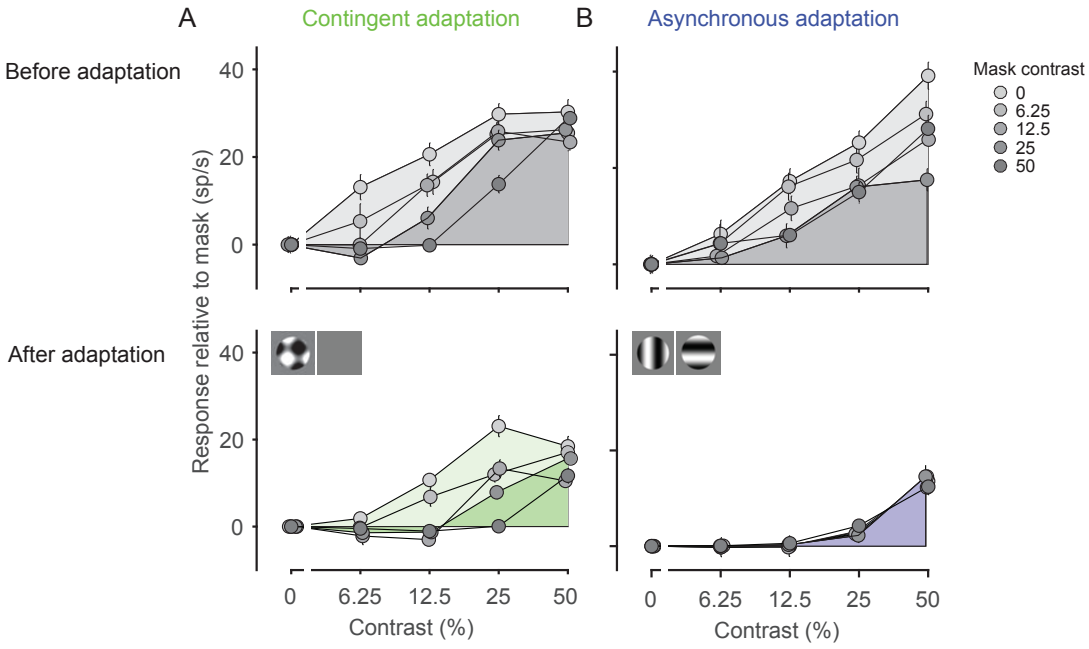

Figure 2

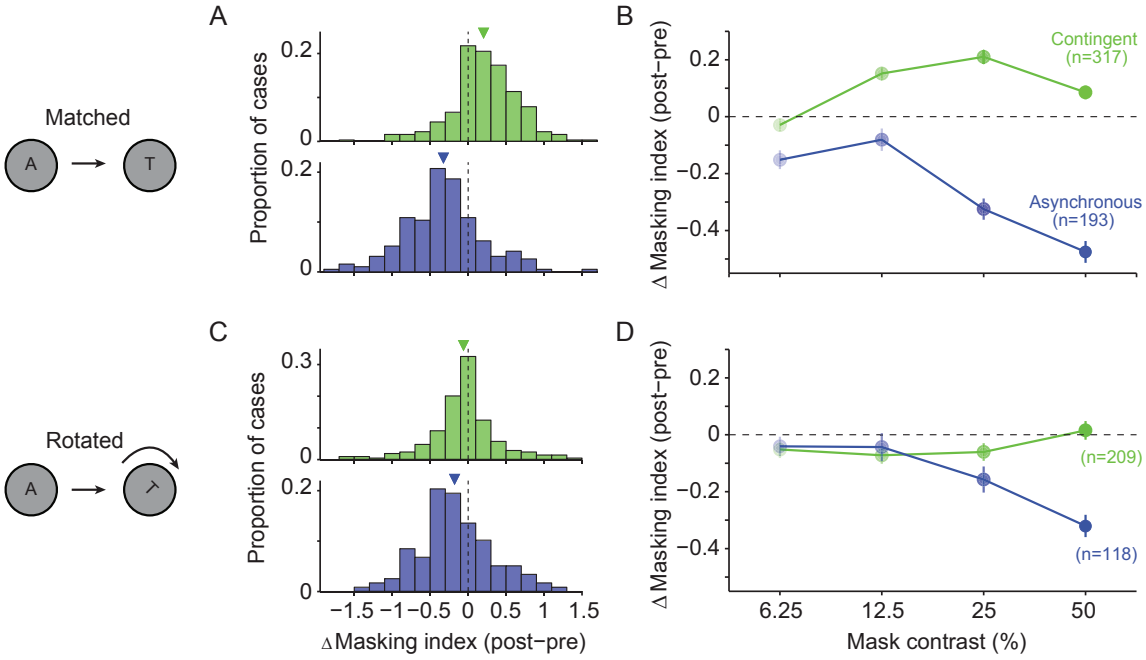

Figure 3

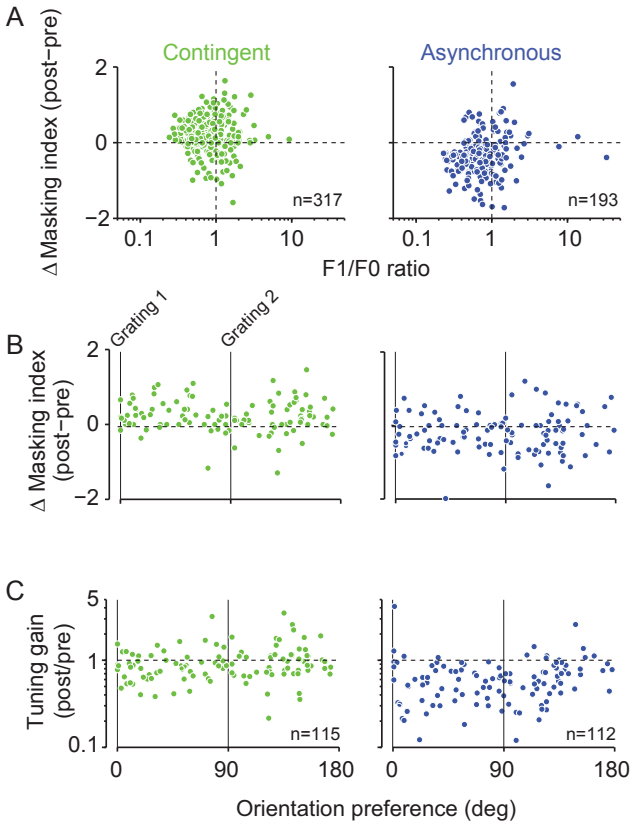

Figure 4

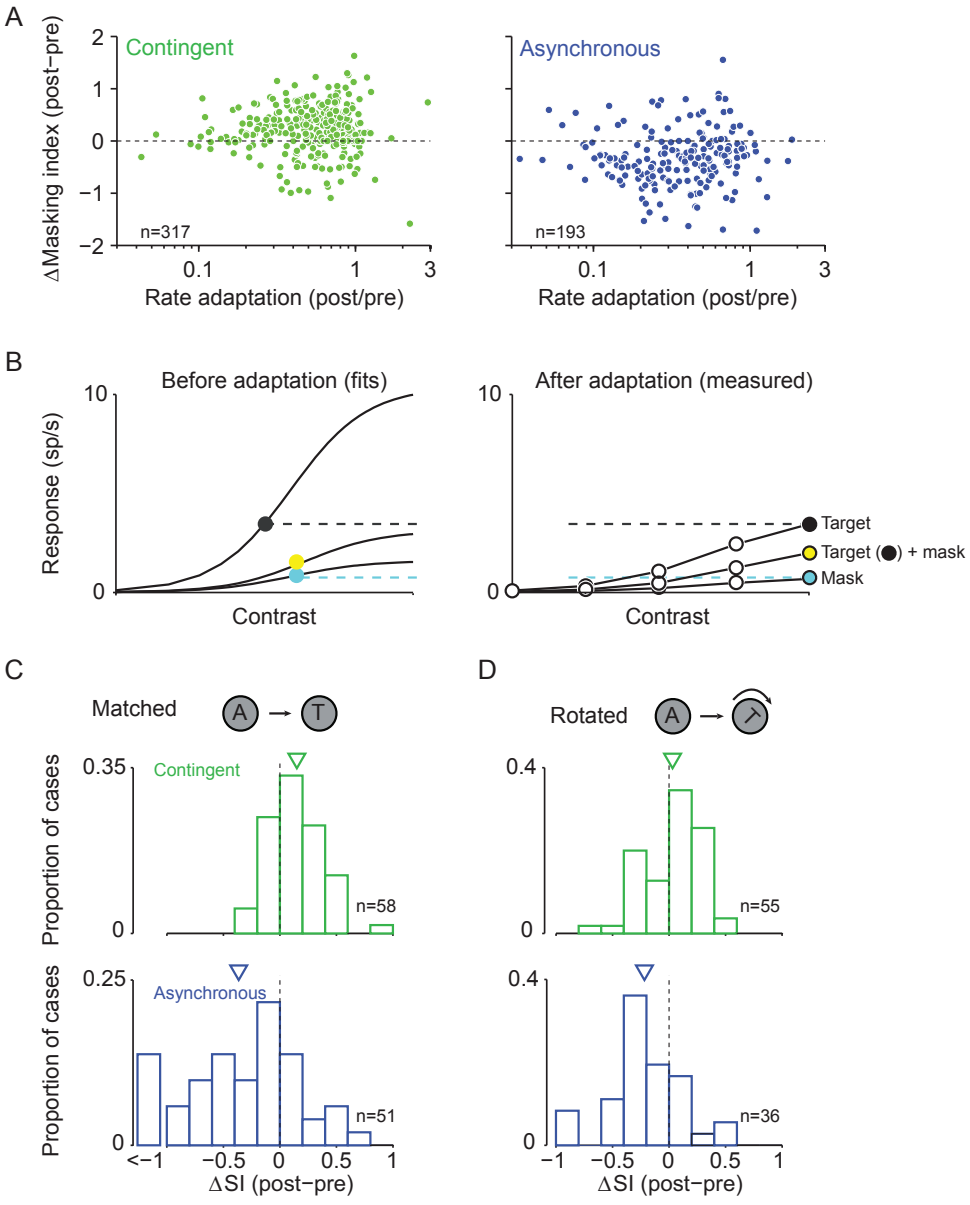

Figure 5

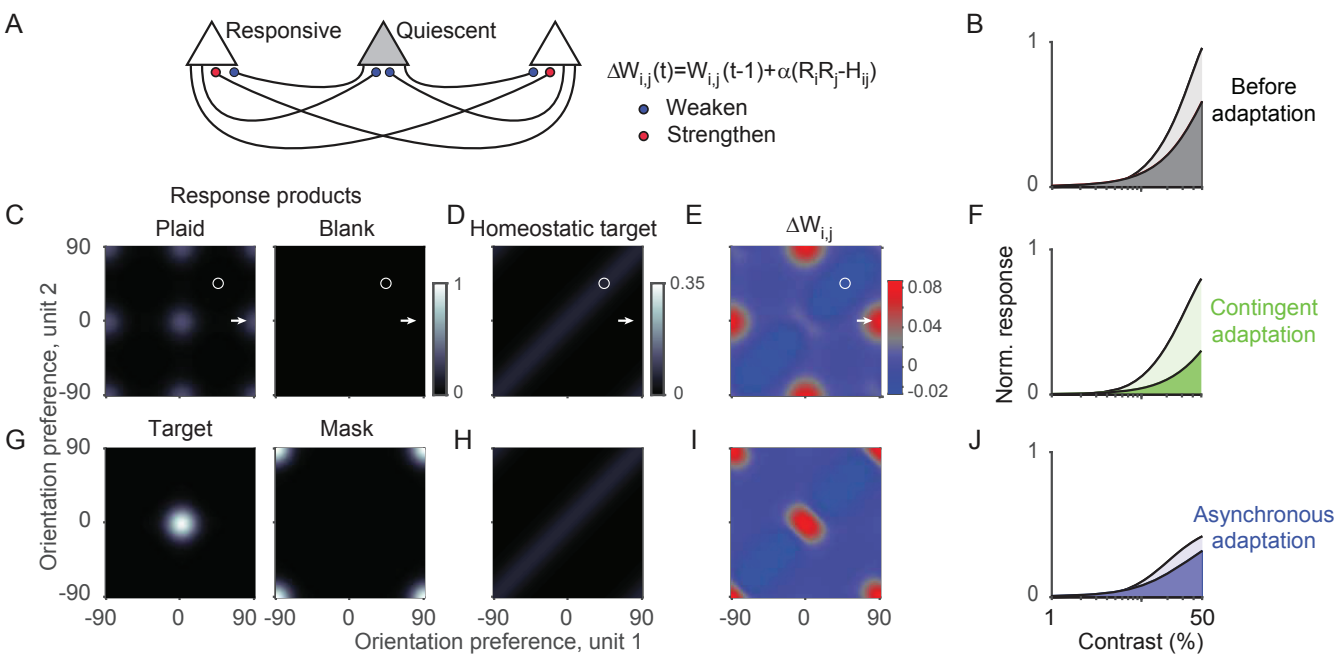

Figure 6

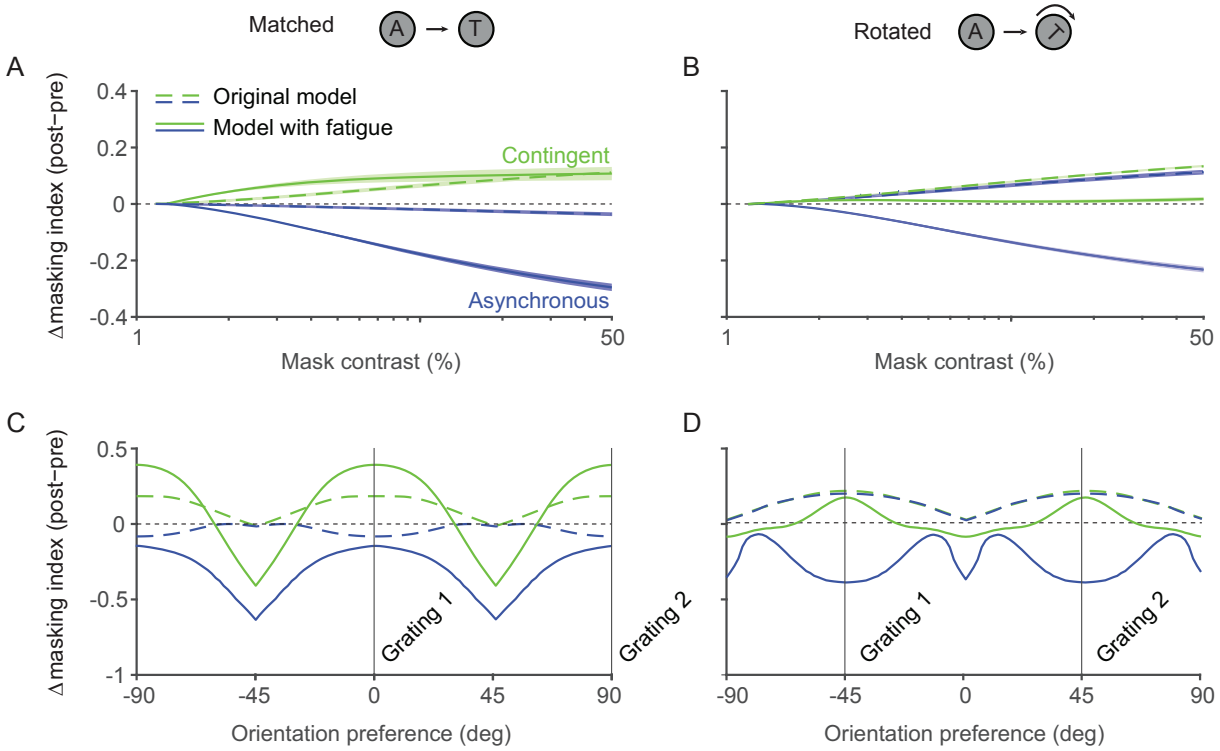

Figure 7

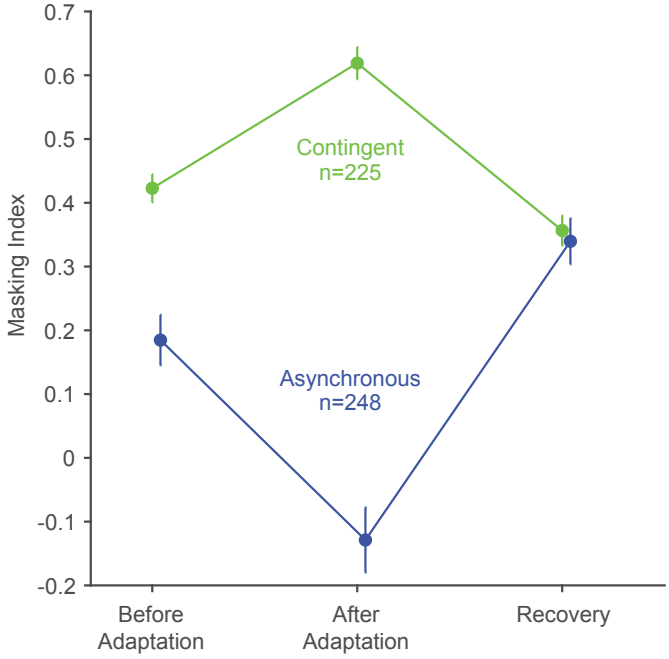

Figure 8